Acta Crystallographica Section B
Structural Science
ISSN 0108-7681

Three differently coloured concomitant polymorphs: synthesis, structure and packing analysis of (4-(3′,5′-dimethyl-1*H*-pyrazol-1′-yl)-6-methyl-2-phenylpyrimidine)dichlorocopper(II)

Eugenia V. Peresypkina,[a]* Mark B. Bushuev,[a] Alexander V. Virovets,[a] Victor P. Krivopalov,[b] Ludmila G. Lavrenova[a] and Stanislav V. Larionov[a]

[a]A. V. Nikolaev Institute of Inorganic Chemistry, Siberian Branch of the Russian Academy of Sciences, Novosibirsk, Russia, and [b]N. N. Vorozhtsov Novosibirsk Institute of Organic Chemistry, Siberian Branch of the Russian Academy of Sciences, Novosibirsk, Russia

Correspondence e-mail: peresyp@che.nsk.su

Received 15 October 2004
Accepted 13 December 2004

Dedicated to Professor Vladislav A. Blatov on the occasion of his 40th birthday

A novel pyrazolylpyrimidine ligand (*L*) and its complex $CuLCl_2$ were prepared and structurally characterized. The simultaneous crystallization of three polymorphs of $CuLCl_2$, green (G), emerald green (EG) and orange (O), was discovered. The molecular structures vary only slightly between the three forms. The Cu atom forms four coordinate bonds with the two N and two Cl atoms, and a shortened Cu···H contact with an H atom of the phenyl ring in *L*. The structural difference between polymorphs was analyzed with the boundary surfaces of molecular Voronoi–Dirichlet polyhedra. The difference in colour of the polymorphs is likely to be due to the different π–π stackings. There is no stacking in the G modification, but EG and O polymorphs demonstrate face-to-face and slipped stacking, resulting in dimers and infinite chains, respectively. The EG and O polymorphs are packed according to the hexagonal close-packing motif, while in G no special topology is found.

1. Introduction

Pyrazolylpyrimidines are of interest from various viewpoints. They demonstrate biological activities as cytoprotectors (Ikeda *et al.*, 1996, 1997), analogues of TNF-α signalling modulators (Sneddon *et al.*, 2001), InhA inhibitors (Staveski *et al.*, 2001), cardiotonic agents (Sedereviciute *et al.*, 1998) and antitumor agents (Ejima *et al.*, 1996). Pyrazolylpyrimidines also demonstrate pesticidal properties (Fischer *et al.*, 2002; Grote *et al.*, 2002; Selby *et al.*, 2002). 4-Methoxy-2-(5-methoxy-3-methyl-1*H*-pyrazol-1-yl)-6-methylpyrimidine (mepirizole) is used as an analgesic and an anti-inflammatory agent (Oshima *et al.*, 1969). These compounds can act as ligands for the synthesis of coordination compounds because of the presence of donor atoms (Gomez de la Torre *et al.*, 2000, and references therein; Escriva *et al.*, 2003, and references therein; Elguero *et al.*, 2001, and references therein). By varying the number and the position of the substituents in the pyrazolylpyrimidines, coordination compounds with catalytic (Druzhkov *et al.*, 2004) or interesting magnetic properties (Escriva *et al.*, 2003) can be obtained. Pyrazolylpyrimidines are also very appealing ligands in the design of spin-crossover systems similar to those obtained earlier with the related azine systems pyrazolylpyrazines and pyrazolylpyridines (Money *et al.*, 2004, and references therein).

Recently we have prepared a novel ligand with a developed π-system, 4-(3′,5′-dimethyl-1*H*-pyrazol-1′-yl)-6-methyl-2-phenylpyrimidyne [*L*, (1)], and have been investigating its complexes with transition metals.

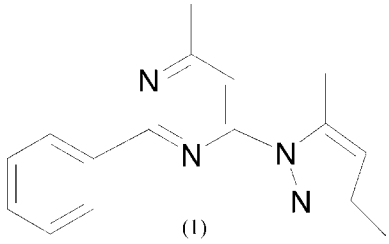

(1)

The structure of (1) is expected to demonstrate π–π interactions, resulting in a stacked crystal structure. We are interested in the effects on π–π interactions if complexes of *L* with 3*d* transition metals are studied, especially with copper(II) for which square-planar coordination is possible resulting in virtually planar complexes. During the crystallization of complexes of $CuCl_2$ with *L*, $CuLCl_2$ (2), we have observed the unexpected phenomenon of the simultaneous crystallization of three differently coloured polymorphic modifications. This publication is devoted to the structural analysis of (1) and (2), and the analysis of any possible structural reasons for 'colour polymorphism' (Bernstein *et al.*, 1999, and references therein). The latter is of special interest because in the literature the main attention is usually focused on the formal description of crystal structures or thermodynamical aspects, but not to the detailed comparative crystallochemical analysis of polymorphs.

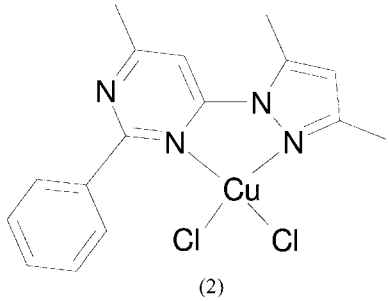

(2)

2. Experimental

2.1. General remarks

All commercially available reagents were used without further purification. The copper content was determined by complexonometric titration, the samples being decomposed in a 1:1 mixture of concentrated H_2SO_4 and HNO_3. The CHN analyses were performed with a Carlo–Erba analyser using the standard procedure.

2.2. Synthesis of 4-(3′,5′-dimethyl-1*H*-pyrazol-1′-yl)-6-methyl-2-phenylpyrimidine [*L*, (1)]

A solution of 4-hydrazino-6-methyl-2-phenylpyrimidine (15 mmol) and acetylacetone (22 mmol) in ethanol (15 ml) was refluxed for 6 h. The solid obtained after cooling the mixture in a refrigerator was filtered off, washed with ethanol and dried to give 4-(3′,5′-dimethyl-1*H*-pyrazol-1′-yl)-6-methyl-2-phenylpyrimidine, yield 90%, m.p. 382–383 K. High-resolution mass spectrum (EI, 70 eV), *m*/*z*: calc. for $C_{16}H_{16}N_4$ 264.1374; found 264.1434. ^{1}H NMR (200.13 MHz, CDCl3): δ 2.30 (3H, d, $J \simeq 1$ Hz, Me-3′), 2.59 (3H, d, $J \simeq 1$ Hz, Me-5′), 2.86 (3H, s, Me-6), 6.04 (1H, br s, H-4′), 7.39–7.57 (3H, m, Ph), 7.65 (1H, s, H-5), 8.33–8.52 (2H, m, Ph).

Crystallization of (1) from a solution in CH_3CN with a small amount of ethanol resulted in thin-fibre colourless crystals that show very weak diffraction.

2.3. Synthesis of $CuLCl_2$ (2)

A hot solution of *L* (1 mmol) in 15 ml of 2-propanol was added slowly with stirring to a hot solution of $CuCl_2{\cdot}2H_2O$ (1 mmol) in 5 ml of 2-propanol. A greenish-yellow precipitate was formed after *ca* 1 min. After stirring for 2 h with heating the precipitate was separated from the mother liquor by filtration and carefully washed according to the following technique. 2-Propanol (5 ml) was added to the freshly prepared precipitate and the mixture was stirred with heating for 1 h. After that the precipitate was filtered off, additionally washed with a small amount of 2-propanol and dried in ambient air. Yield 65%. Anal: found (calc.) for $C_{16}H_{16}N_4Cl_2Cu$: C 48.4 (48.2), H 4.1 (4.0), N 14.1 (14.0), Cu 15.6 (15.9)%.

2.4. Crystallization of three different polymorphic modifications of (2)

A small amount of the powder sample of (2) was dissolved in a mixture of 2-propanol and acetonitrile (*ca* 2:1) with intense heating. When we left the hot solution to cool down at room temperature, within a few hours clear green plate crys-

Figure 1
Crystals of the three polymorphic modifications of (2).

Table 1
Experimental data for 4-(3′,5′-dimethyl-1*H*-pyrazol-1′-yl)-6-methyl-2-phenylpyrimidyne and its copper chloride complex.

	(1)	(2O)	(2EG)	(2G)
Crystal data				
Chemical formula	$C_{16}H_{16}N_4$	$C_{16}H_{16}Cl_2CuN_4$	$C_{16}H_{16}Cl_2CuN_4$	$C_{16}H_{16}Cl_2CuN_4$
M_r	264.33	398.77	398.77	98.77
Cell setting, space group	Orthorhombic, *Pna*2(1)	Monoclinic, $P2_1/n$	Orthorhombic, *Pbca*	Monoclinic, $P2_1/c$
a, *b*, *c* (Å)	19.499 (3), 4.7884 (6), 15.106 (2)	9.7652 (6), 18.7631 (10), 9.8115 (4)	11.6899 (6), 14.9843 (8), 19.2115 (9)	7.2156 (3), 11.6522 (4), 20.3956 (8)
β (°)	90	108.5440 (10)	90	99.8410 (10)
V (Å^3)	1410.5 (3)	1704.38 (16)	3365.2 (3)	1689.58 (11)
Z	4	4	8	4
Dx (Mg m^{-3})	1.245	1.554	1.574	1.568
Radiation type	Mo $K\alpha$	Mo $K\alpha$	Mo $K\alpha$	Mo $K\alpha$
No. of reflections for cell parameters	1009	5800	4601	3896
θ range (°)	2.5–22.1	2.2–27.4	2.5–30.5	2.7–30.1
μ (mm^{-1})	0.08	1.60	1.62	1.61
Temperature (K)	293 (2)	293 (2)	293 (2)	293 (2)
Crystal form, colour	Lath, colourless	Prism, orange	Elongated prism, emerald green	Plate, green
Crystal size (mm)	0.59 × 0.05 × 0.03	0.31 × 0.17 × 0.12	0.33 × 0.10 × 0.09	0.54 × 0.23 × 0.04
Data collection				
Diffractometer	Bruker–Nonius X8Apex CCD area detector	Bruker–Nonius X8Apex CCD area detector	Bruker–Nonius X8Apex CCD area detector	Bruker–Nonius X8Apex CCD area detector
Data collection method	φ-scans	φ-scans	φ-scans	φ-scans
Absorption correction	None	Empirical (using intensity measurements)	Empirical (using intensity measurements)	Empirical (using intensity measurements)
T_{min}	–	0.721	0.657	0.645
T_{max}	–	0.820	0.86	0.941
No. of measured, independent and observed reflections	9460, 2221, 885	12 988, 3915, 3240	17 334, 5379, 3611	10 578, 5033, 3781
Criterion for observed reflections	$I > 2\sigma(I)$	$I > 2\sigma(I)$	$I > 2\sigma(I)$	$I > 2\sigma(I)$
R_{int}	0.083	0.019	0.024	0.016
θ_{max} (°)	30.6	27.6	32.4	32.5
Range of *h*, *k*, *l*	$-27 \Rightarrow h \Rightarrow 27$ $-3 \Rightarrow k \Rightarrow 6$ $-21 \Rightarrow l \Rightarrow 21$	$-12 \Rightarrow h \Rightarrow 12$ $-24 \Rightarrow k \Rightarrow 24$ $-12 \Rightarrow l \Rightarrow 8$	$-16 \Rightarrow h \Rightarrow 17$ $-17 \Rightarrow k \Rightarrow 22$ $-26 \Rightarrow l$ 15	$-10 \Rightarrow h \Rightarrow 9$ $-10 \Rightarrow k \Rightarrow 16$ $-30 \Rightarrow l \Rightarrow 29$
Refinement				
Refinement on	F^2	F^2	F^2	F^2
$R[F^2 > 2\sigma(F^2)]$, $wR(F^2)$, S	0.059, 0.181, 0.91	0.029, 0.088, 1.10	0.032, 0.098, 0.86	0.033, 0.107, 0.94
No. of reflections	2221	3915	5379	5033
No. of parameters	182	209	208	208
H-atom treatment	Constrained refinement	Constrained refinement	Constrained refinement	Constrained refinement
Weighting scheme	$w = 1/[\sigma^2(F_o^2) + (0.0847P)^2]$, where $P = (F_o^2 + 2F_c^2)/3$	$w = 1/[\sigma^2(F_o^2) + (0.0507P)^2 + 0.2601P]$, where $P = (F_o^2 + 2F_c^2)/3$	$w = 1/[\sigma^2(F_o^2) + (0.053P)^2 + 2.2199P]$, where $P = (F_o^2 + 2F_c^2)/3$	$w = 1/[\sigma_2(F_o^2) + (0.0633P)^2 + 0.6674P]$, where $P = (F_o^2 + 2F_c^2)/3$
$(\Delta/\sigma)_{max}$	< 0.0001	0.002	0.001	0.002
$\Delta\rho_{max}$, $\Delta\rho_{min}$ (e Å^{-3})	0.14, −0.15	0.38, −0.28	0.49, −0.43	0.49, −0.31
Extinction method	–	*SHELXL*	–	–
Extinction coefficient	–	0.0021 (6)	–	–

Computer programs used: Bruker *APEX*2, Bruker *SAINT*, Bruker *SADABS*, *SHELXS*86 (Sheldrick, 1990), *SHELXL*97 (Sheldrick, 1998).

tals (2G) appeared. After 24 h at room temperature these crystals slowly disappeared but two new phases appeared: emerald green prismatic (2EG) and orange flattened prismatic crystals [(2O), Fig. 1]. X-ray structural analysis shows that all three types of crystals have the same composition, Cu*L*Cl$_2$, and therefore correspond to the different solvent-free polymorpic modifications of (2). Sometimes emerald green crystals formed agglomerates with orange crystals on the surface. When almost all the solvent had evaporated we observed a comparable amount of orange and emerald green phases with a very small amount of light-green crystals, mainly in the form of agglomerates. Crystallization from pure acetonitrile showed slightly different behaviour: first the green phase was crystallized and then, after approximately 36 h, the first orange crystals appeared with only a few crystals of emerald green polymorph. Taking into account the sequence of crystallization, we believe that the green phase is probably metastable at room temperature (2G). The emerald green and orange phases may be stable at room temperature but the orange phase is less kinetically preferable than green, because in a series of crystallizations the orange crystals appeared after the emerald green crystals. Note that the fine powder sample

of (2) precipitated during the synthesis corresponds to the (2G) modification according to X-ray powder diffraction data.

Low-temperature single-crystal studies of all three modifications of (2) in the temperature range 300–90 K showed no phase transitions.

2.5. Crystallographic and crystallochemical studies

The crystal structures of (1) and all the three types of crystals of (2) were determined by single-crystal X-ray structural analysis. Crystallographic data, details of structure solution and refinement are given in Table 1. [1] Packing coefficients were calculated using the program *KPACK* (Virovets & Podberezskaya, 1992) using 1000 test points per cubic Å and the following van der Waals radii (Å): C 1.71, H 1.15, N 1.50, Cl 1.90 (Zefirov, 1997). For the Cu atom a metallic radius of 1.28 Å was taken. The environment of the Cu atoms, the geometry of a molecule and the topology of molecular packings were investigated using *Dirichlet*, *ADS* and *IsoTest* programs from the *TOPOS*3.2 program set (Blatov *et al.*, 2000). The algorithms are based on the Voronoi–Dirichlet partition of crystalline space, where each atom is represented by a convex Voronoi–Dirichlet polyhedron (VDP; Blatov & Serezhkin, 2000). Atoms belonging to the same molecule comprise a molecular VDP, which is always non-convex (Ovchinnikov *et al.*, 1995; Peresypkina & Blatov, 1999). Peresypkina & Blatov (2000*a*,*b*, 2002) showed that a molecule could be assigned with its molecular VDP and some characteristics of the molecule could then be calculated, such as molecular coordination numbers, area of intermolecular boundary surface and its relative solid angle *etc.* This approach also allows the general motif of the molecular arrangements in crystals to be analysed (using coordination sequences; O'Keeffe, 1995) and the degree of distortion, G_3 (or regularity of molecular arrangement; Blatov, 2001; Peresypkina & Blatov, 2002). The smaller the G_3 value, the more regular the molecular lattice. Note that among periodic lattices the lowest value G_3 = 0.07854 corresponds to the b.c.c. (body-centred cubic) lattice, while G_3 = 0.07875 characterizes the close packings.

3. Discussion

A chemical compound can generally be described as polymorphic 'if it forms two or more crystalline phases differing in atomic arrangements' (Wells, 1986). For molecular crystals we should add that polymorphs must differ in the crystal packing of the same molecules (Bernstein *et al.*, 1999). Sometimes two or more polymorphs appear at the same time from the same mother liquor (so-called concomitant polymorphs; Bernstein *et al.*, 1999, and references therein). The concomitant polymorphs sometimes have different colours, but the origin of this phenomenon, called 'colour polymorphism' or 'chromatomorphism', is not always clear and may be due to different reasons (Bernstein, 1987, 1993; Bernstein *et al.*, 1999; Yu, Stephenson *et al.*, 2000; Yu, 2002). There are at least three possible reasons for the different colours of the polymorphs of (2): a different molecular conformation, a different environment of Cu atoms in the crystal or the different packing motifs that can theoretically influence the electronic structure of molecules if the intermolecular interactions, *e.g.* interaction between π-systems, are strong enough. Let us first analyse the molecular geometry of (1) and (2).

3.1. Molecular geometry

Molecules (1) and (2) are shown in Figs. 2(*a*) and (*b*) with the main geometrical parameters being given in Table 2. The pyrazole, pyrimidine and phenyl rings are planar to within 0.005 Å. Bond distances and valence angles in the organic part of the molecular complex for all three polymorphic modifications are very close to those for the free ligand, but their conformations are different. First the relative orientations of the pyrazole and pyrimidine rings in (1) and (2) are opposite (Figs. 2*a* and *b*; Table 2). Obviously this is a requirement for a ligand to be coordinated to the Cu atom. The relative orien-

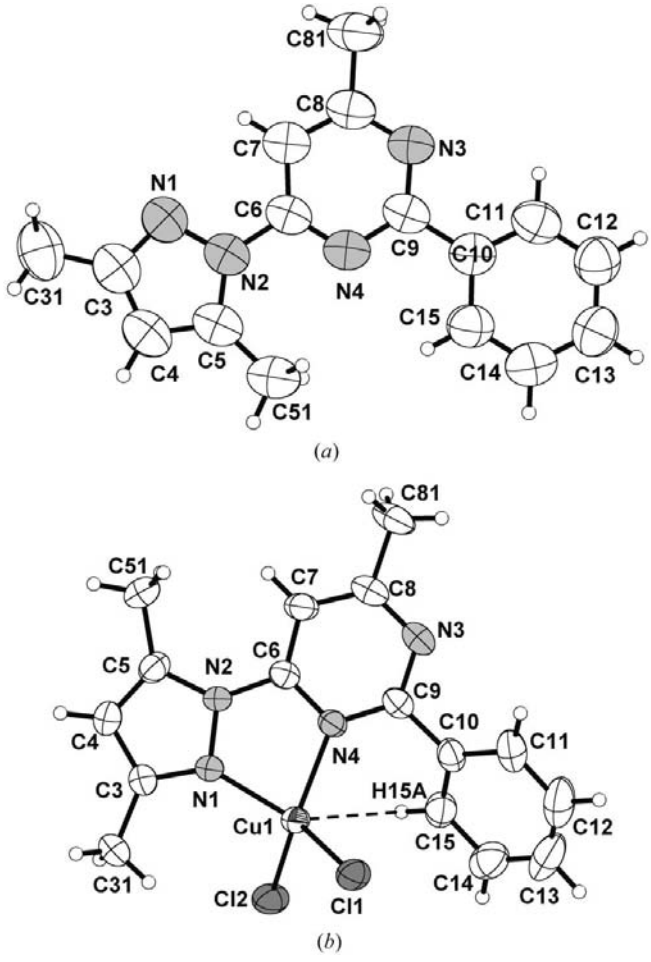

Figure 2
Molecules in (*a*) (1) and (*b*) (2O) with displacement ellipsoids at the 50% probability level. The numbering schemes in (2EG) and (2G) are identical. The shortened Cu···H contact in (2) is shown by a dashed line.

[1] Supplementary data for this paper are available from the IUCr electronic archives (Reference: AV5023). Services for accessing these data are described at the back of the journal.

Table 2
Some geometrical characteristics of molecules (1) and (2O), (2EG) and (2G).

	(1)	(2O)	(2EG)	(2G)
Bond length (Å)				
Cu—Cl1	–	2.2219 (5)	2.2307 (6)	2.2147 (6)
Cu—Cl2	–	2.2008 (5)	2.1836 (6)	2.1898 (6)
Cu—N1	–	1.9679 (15)	1.9938(16)	2.0011 (16)
Cu—N4	–	2.0348 (14)	2.0098 (15)	2.0259 (15)
N1—N2	1.374 (5)	1.378 (2)	1.385 (2)	1.376 (2)
C3—C4	1.393 (6)	1.400 (3)	1.393 (3)	1.399 (3)
C3—N1	1.325 (6)	1.326 (2)	1.334 (2)	1.335 (2)
C4—C5	1.371 (6)	1.357 (3)	1.365 (3)	1.360 (3)
C5—N2	1.376 (5)	1.383 (2)	1.377 (2)	1.374 (2)
C6—C7	1.393 (6)	1.376 (2)	1.383 (2)	1.366 (3)
C6—N2	1.415 (5)	1.398 (2)	1.401 (2)	1.410 (2)
C6—N4	1.309 (5)	1.347 (2)	1.346 (2)	1.346 (2)
C7—C8	1.394 (6)	1.384 (3)	1.395 (3)	1.395 (3)
C8—N3	1.347 (5)	1.346 (3)	1.349 (3)	1.345 (3)
C9—C10	1.491 (6)	1.477 (3)	1.480 (3)	1.480 (3)
C9—N3	1.325 (5)	1.332 (2)	1.331 (2)	1.326 (3)
C9—N4	1.349 (5)	1.347 (2)	1.342 (2)	1.348 (2)
Valence angle (°)				
Cl2—Cu1—Cl1	–	104.42 (2)	103.09 (2)	102.57 (3)
N1—Cu1—Cl1	–	132.22 (5)	136.93 (5)	137.72 (5)
N1—Cu1—Cl2	–	100.81 (5)	101.56 (5)	101.34 (5)
N1—Cu1—N4	–	79.95 (6)	79.01(6)	79.74 (6)
N4–Cu1–Cl1	–	104.31 (4)	96.23 (5)	96.45 (5)
N4—Cu1—Cl2	–	139.41 (5)	149.38 (5)	148.86 (5)
Torsion angle (°)				
N1—N2—C6—N4 (φ_1)	−177.4 (3)	2.8 (2)	−1.5 (2)	−1.5 (2)
N4—C9—C10—C15 (φ_2)	6.4 (5)	38.6 (3)	35.2 (3)	32.0 (3)
Deviation of atom from the N1—N2—C6—N4 plane (Å)				
Cu1	–	−0.050 (3)	−0.503 (3)	−0.420 (3)
Cl1	–	−1.707 (5)	−2.342 (4)	−2.172 (4)
Cl2	–	1.328 (5)	0.061 (5)	0.242 (5)

tations of the phenyl and pyrimidine rings are therefore also different in (1) and (2). In the ligand the torsion angle N4—C9—C10—C15 (φ_2) is much smaller than in the complex (Table 2). Obviously this is because of the steric problems between the Cu atom and one of the H atoms of the phenyl ring resulting in relatively short Cu···H intramolecular contacts (Fig. 2*b*, Table 3).

From Table 2 we can see that the torsion angle N1—N2—C6—N4 (φ_1) of the pyrazole ring in rotation with respect to the pyrimidine ring varies within 7 Å in different polymorphs. The Cu—Cl and Cu—N distances are the same to within 0.03 Å, while the deviations of the Cu atom from the chelate ring are the same to within 0.05–0.5 Å. It seems unbelievable that such small changes in geometry can cause such a difference in the electronic state of a molecule (for example, by the energy of conjugation) to turn the green colour into orange. For instance, in the reported polymorphic system of 5-methyl-2-[(2-nitriphenyl)amino]-3-thiophenecarbonitrile (Yu, 2002), in order to change the colour of the crystals from yellow to orange or from orange to red–orange, the torsion angles must have changed by 51.5 and 17.7°, respectively, while difference of *ca* 7 Å did not yield another colour. Of course, these slight differences in molecular conformations may contribute to changes in colours (Yu, Reutzel-Edens & Mitchell, 2000), but they are not anticipated to be dominant.

3.2. Additional coordination to Cu atoms

Another possible reason for the difference in electronic state of the molecule is that in the crystal packing there is an atom or atoms that make additional short contact(s) with Cu atoms. We have analysed the nearest environment of the Cu atoms using their VDPs (Blatov & Serezhkin, 2000). All three polymorphs appeared to be the same (Table 3). The Cu atoms form four covalent bonds with ligands and one short intramolecular Cu···H contact with the H atom of the phenyl ring. In addition, there are two (2O) or three [(2EG) and (G)] Cu···H intermolecular contacts which are quite long, > 3.1 Å. The volumes of the VDPs of Cu atoms and the degree of their sphericity (G_3) are similar.

3.3. Crystal packings

Finally, let us turn to the careful analysis of the crystal packings of (2), because the different molecular environment and thus the peculiarities of the intermolecular interactions in the crystal packings of the polymorphs are likely to be the reason for the change in their colours. Moreover, crystallochemical analysis of polymorphic systems can reveal the structural features in molecular crystals of the same composition and may be useful in understanding their 'structure–property' relations (Bernstein *et al.*, 1999; Yu, 2002). Note that one can semi-qualitatively estimate the relative efficiency of the intermolecular interactions between a molecule and its nearest neighbours using molecular VDPs. An example of a molecular VDP is shown in Fig. 3. The surface of

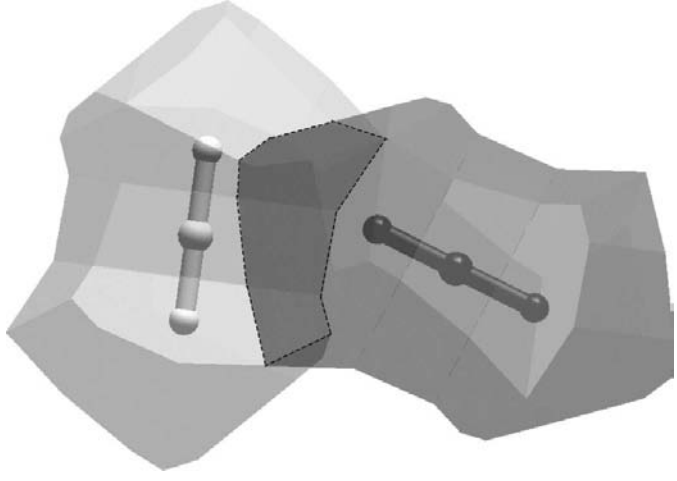

Figure 3
An example of the molecular Voronoi–Dirichlet polyhedra of two neighbouring molecules in the crystal structure of CO_2. The boundary surface between the molecules is shown by a dashed line.

Table 3
The nearest environment of the Cu atom in (2).

	(2O)	(2EG)	(2G)
Volume of Cu VDP	13.47	13.09	13.52
G_3 of Cu VDP	0.0936	0.0895	0.0901
Coordination number of Cu	4 + 3	4 + 4	4 + 4
Distances from Cu to surrounding atoms (Å) with corresponding solid angle, % of 4π steradian†	1.968, 20.40 – N1 2.035, 19.26 – N4 2.201, 19.70 – Cl2 2.222, 20.20 – Cl1 2.612, 11.85 – H(15*A*) 3.137, 3.45 – H31*C* 3.201, 5.14 – H81*B*′	1.994, 20.39 – N1 2.010, 18.30 – N4 2.184, 19.76 – Cl2 2.231, 19.02 – Cl1 2.608, 11.20 – H(15*A*) 3.241, 3.27 – H81*C*′ 3.373, 3.72 – H7*A*′ 3.375, 4.33 – H81*B*′	2.001, 20.67 – N1 2.026, 18.32 – N4 2.190, 20.50 – Cl2 2.215, 19.2 – Cl1 2.701, 10.85 – H(15*A*) 3.385, 2.48 – H81 *C*′ 3.392, 4.34 – H81*B*′ 3.422, 3.61 – H7*A*′

† Only interatomic contacts with a solid angle >1.5% of 4π-steradian are taken into account (Blatov & Serezhkin, 2000).

a molecular VDP consists of a set of VDP faces. Each of them corresponds to an interaction between atoms belonging to different molecules. VDP faces between a molecule and one of the molecules of its nearest environment form a so-called boundary surface (Fig. 3; Ovchinnikov *et al.*, 1995), which corresponds to the molecule–molecule interaction in the crystal structure. The number of boundary surfaces thus gives the molecular coordination number (MCN). The stronger the intermolecular interactions, the larger the boundary surface. The size of the boundary surface can be estimated most accurately not by its area, but by the corresponding solid angle (Ω_{mol}; Peresypkina & Blatov, 2000*a*), which is usually presented as a percentage of the total solid angle for all intermolecular contacts made by a given molecule and allows correct comparison. In fact, the size of a boundary surface depends on the number of nearest molecules and on the molecular shape in the context of being more or less spherical or rather elongated. In the case of spherical molecules, its packing usually tends to be uniform (Peresypkina & Blatov, 2000*b*). This means that the average estimated Ω_{mol} is equal to 100% divided by MCN, which is *ca* 7% for MCN = 14 (Table 4). For a non-spherical molecule the boundary surface should vary, which is difficult to predict. However, in the case of different packing patterns of the same molecule this approach allows us to reveal some interesting packing features caused by different intermolecular interactions. The geometrical characteristics of the spatial arrangements of molecules are given in Table 4, which show the existence of π–π stacking in some cases. Shorter distances between molecules correspond to a large solid angle value and a huge number of intermolecular contacts, comprising the boundary surface (Fig. 4), showing important molecule–molecule interactions. It can be seen that in (2O) and (2EG) the distances between the molecular centres of gravity are of two types: shortened, *ca* 5 Å, and elongated, > 9 Å. Moreover, in (2O) there are two shortened contacts in comparison with only the one in the case of (2EG). Thus, in (2O) each molecule is surrounded by two molecules in a stack, which in turn also have the same environment (Fig. 5*a*), *i.e.* molecular packing consists of columns of molecules in a slipped stack involving the whole aromatic fragment of the molecule (Janiak, 2000) with alternating cycle–cycle distances (Figs. 4*a* and 6*a*). In (2EG) the structure molecules are joined to dimers (Figs. 4*b*, 5*b* and 6*b*) forming face-to-face π–π stacks involving pyrimidine rings (Janiak, 2000). In the case of (2G) there are no such shortened intermolecular distances (Fig. 6*c*, Table 4); two distances of *ca* 7 Å correspond to relatively small boundary surfaces with a low solid angle value and a small number of contacts involved. In this structure there is no π-stacking (Fig. 4*a*, Table 4) and the nearest molecules are not parallel, but inclined by *ca* 17°. At the same time the crystal packing is not of the herring-bone type that is expected for such systems in the absence of π–π stacking (Janiak, 2000). Note that the presence of π–π stacking resulted in solid angles of the boundary surfaces which are twice the size and can easily be seen without even visualizing the crystal structure.

In the structure of (1) π–π interactions are also present (Fig. 4*d*), resulting in a column of molecules running along the short *b* axis (Fig. 6*d*).

The crystal structures of (2) demonstrate an unusual dependence of the stability of the polymorphs on their densities D_x (Table 1). According to the well known 'density rule' (Bernstein *et al.*, 1999; Gavezzotti & Fillippini, 1995), the higher the density of a polymorph the higher its stability. It is natural to assume that (2EG) and (2O) are more stable polymorphs compared with (2G). However, both green forms have similar densities, which are larger than that of the orange form. In fact, the most stable polymorph (2O) has the lowest density. This contradiction is likely to be caused by the fact that the rule assumes only non-directed van der Waals interactions between the molecules in the crystal. In the case of specifically directed intermolecular interactions, such as hydrogen bonding, exceptions were found (Fridman *et al.*, 2004; Yoshino *et al.*, 1999). The same reason may lead to a lower density orange form, whose packing is strongly influenced by π–π stacking interactions. The correlations are the same for molecular volumes and packing coefficients (Table 4).

It is obvious that the system of molecules with only closed-shell interactions tends to be the most uniform arrangement (Peresypkina & Blatov, 2002). If there is a contribution from directed intermolecular interactions, the tendency may either be overcome or not. This stimulated us to analyse the uniformity of the crystal structure for the polymorphs, in addition to the density and packing coefficients *etc.* One can estimate the uniformity of the arrangement of molecules in the crystal structure with G_3 as the criterion (Conway & Sloane, 1988; Peresypkina & Blatov, 2002). The higher the value of G_3, the less uniform the molecular lattice. The values of G_3 (Table 4) show that the molecular packings of (2EG) and (2G) are of

the same uniformity, but are rather more uniform than the molecular packing of (2O).

At the same time the topological analysis of molecular packings (O'Keeffe, 1995; Peresypkina & Blatov, 2000*b*) of three forms showed that the packing motif in the structure of (2EG) and (2O) polymorphs is h.c.p. (hexagonal close packing), while the metastable (2G) polymorph packing motif has no special topology (Table 4). However, (2EG) and (2O) cannot be called close packed due to the rather low uniformity and packing coefficients. This fact is in accordance with the well known tendency of molecular crystals to form close packings (Kitaigorodskii, 1973) or even to have the distorted packing related to close or b.c.c. packing, as shown by Peresypkina & Blatov (2000*b*, 2002) on a great number of organic and inorganic molecular compounds. Moreover, it seems to be very natural that the more stable (2EG) and (2O) polymorphs strive towards one of the close packing patterns.

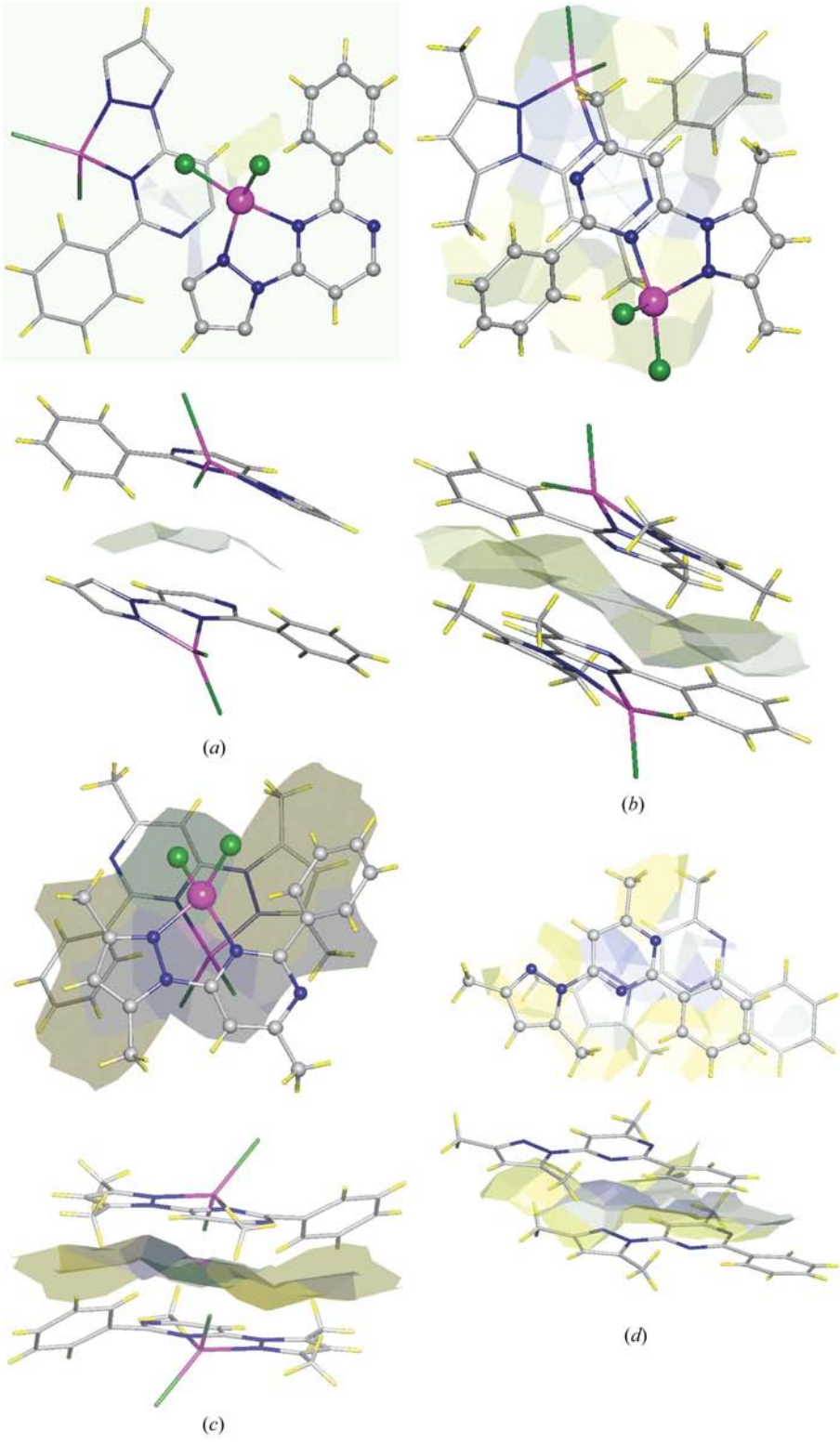

Figure 4
The boundary surfaces between a pair of nearest molecules in the crystal structure of (*a*) (2G), (*b*) (2EG), (*c*) (2O) and (*d*) (1), from two different views.

We believe that it is the π–π stacking interactions which order molecules in (2O) in one dimension, thus forming the chains and yielding molecular packings which are strictly non-uniform. The packing coefficient and density are also rather low. Stacking in (2EG) is limited to dimers and obviously cannot influence the molecular packing so dramatically. Thus, it is reasonable to assume that stacked dimers may be described as the whole particle, because molecules of the dimer are notably closer to each other than to any other molecule and the interactions inside the dimers are stronger than between them. From this point of view the molecular packing of such dimers may only be influenced by van der Waals interactions and thus may lead to an efficient and uniform packing pattern. In fact, according to our calculations the dimers are arranged according to slightly distorted b.c.c. packing (G_3 = 0.0796). This fact may also explain the similarity of (2G) and (2EG) densities.

Studying the molecular structures of (2) can explain the consequences of crystallization of (2G), (2EG) and (2O) polymorphs in terms of ordering of the molecules. The first-precipitating polymorph (2G) has an ordinary crystal structure, where only single molecules are packed by non-directing intermolecular forces, thus its crystallization occurs readily. The structure of the second polymorph (2EG),

Table 4
Geometrical and topological characteristics of crystal packings of (1) and (2).

	(1)	(2O)	(2EG)	(2G)
Geometry				
V/Z (Å^3)	352.6	426.1	420.7	422.4
Packing coefficient	0.656	0.682	0.690	0.687
Molecular coordination number	16	14	14	13
Distances (Å) between the centres of gravity of molecules, with the corresponding number of interatomic contacts, Ω_{mol}, %,† and their multiplicity	4.788, 25, 14.73 × 2; 8.004, 12, 9.56 × 2; 7.952, 7, 7.38 × 2; 9.750, 7, 6.69 × 2; 10.900, 4, 4.35 × 2; 10.824, 3, 2.74 × 2; 11.858, 3, 2.70 × 2	5.403, 47, 26.57; 4.922, 24, 15.34; 9.730, 9, 7.74 × 2; 10.137, 7, 5.51; 8.970, 5, 5.04; 10.387, 5, 4.55 × 2; 12.298, 5, 4.14 × 2; 11.432, 4, 3.84 × 2; 10.796, 4, 3.51 × 2	5.697, 36, 21.91; 7.011, 23, 14.86 × 2; 9.813, 8, 8.14 × 2; 10.645, 7, 4.77 × 2; 10.212, 7, 4.55 × 2; 12.748, 4, 2.93 × 2; 11.690, 3, 2.54 × 2	7.160, 21, 13.52 × 2; 7.065, 17, 12.70 × 2; 10.703, 11, 11.57; 10.236, 10, 6.27 × 2; 9.688, 5, 4.61; 11.476, 7, 4.08 × 2; 11.652, 4, 2.90 × 2; 13.078, 3, 2.69
Average distance (Å) between {N1, N2, N4, C6} planes in the stack	3.45	3.63, 4.61	3.58	No stacking
Topology				
Topology of molecular lattice	Hexagonal primitive	h.c.p.	h.c.p.	No special topology
G_3 of molecular lattice‡	0.09644	0.09147	0.08649	0.08647

† Ω_{mol} is quoted as a percentage of the total solid angle corresponding to all the intermolecular contacts of a reference molecule. ‡ The uniformity criterion for molecular lattices; the larger the G_3 value the more uniform the lattice. Usually G_3 values are in the range from 0.07854 (regular b.c.c.) and 0.07876 (regular close packing) to infinity, but rarely $G_3 > 0.1$ (Blatov *et al.*, 2000; Peresypkina & Blatov, 2002).

consisting of stacked dimers, demands more time to reach an appropriate molecular arrangement during further crystallization. From this viewpoint the completely stacked structure of the polymorph (2O) should appear last. This consequence of crystallization has been realised from 2-propanol/acetonitrile solvent. In the case of pure acetonitrile the sequence has changed, yielding mainly (2G) and then (2O). This could happen because of the capability of acetonitrile to somehow participate in the ordering of molecules of (2) due to its own π-system.

4. Conclusion

The *TOPOS* program set is shown and may be used to efficiently reveal the π–π stacking in crystal structures of aromatic systems by means of the Voronoi–Dirichlet partition

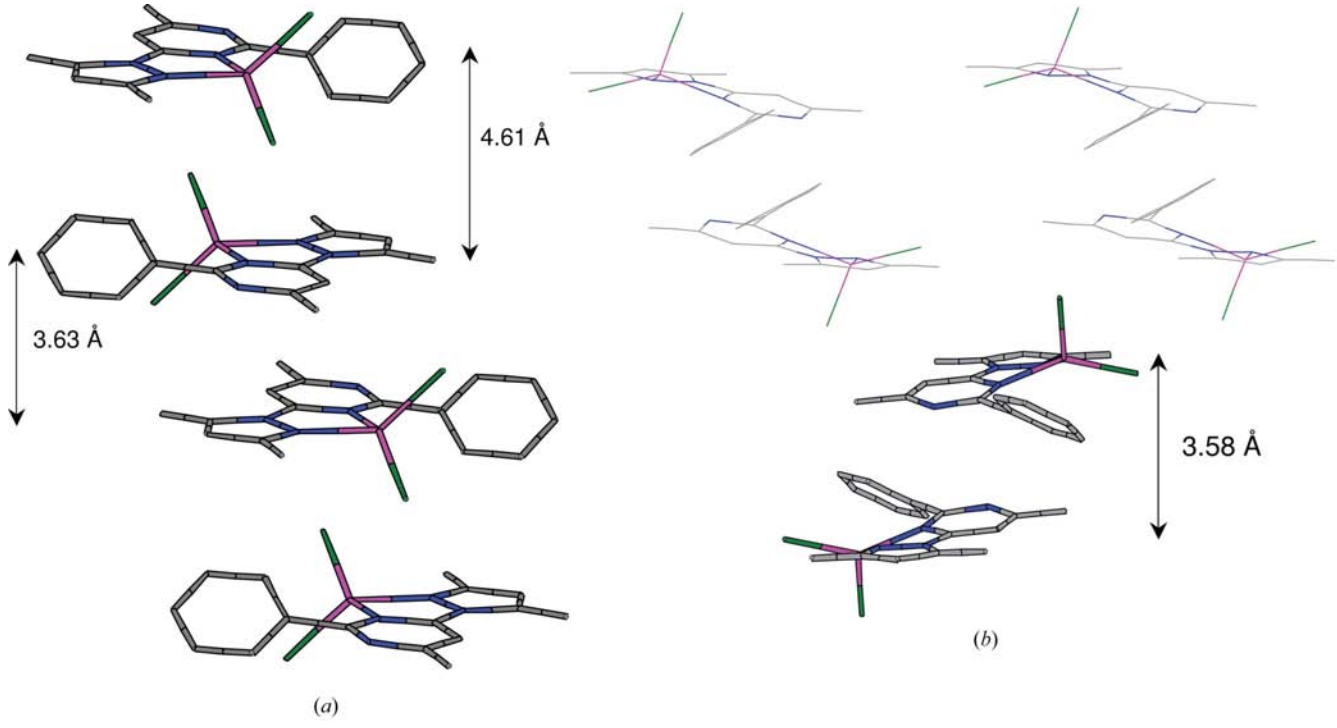

Figure 5
The different ways of π–π stacking: (*a*) chain of molecules in (2O) and (*b*) the dimer in (2EG). Molecules in the stack are shown in bold.

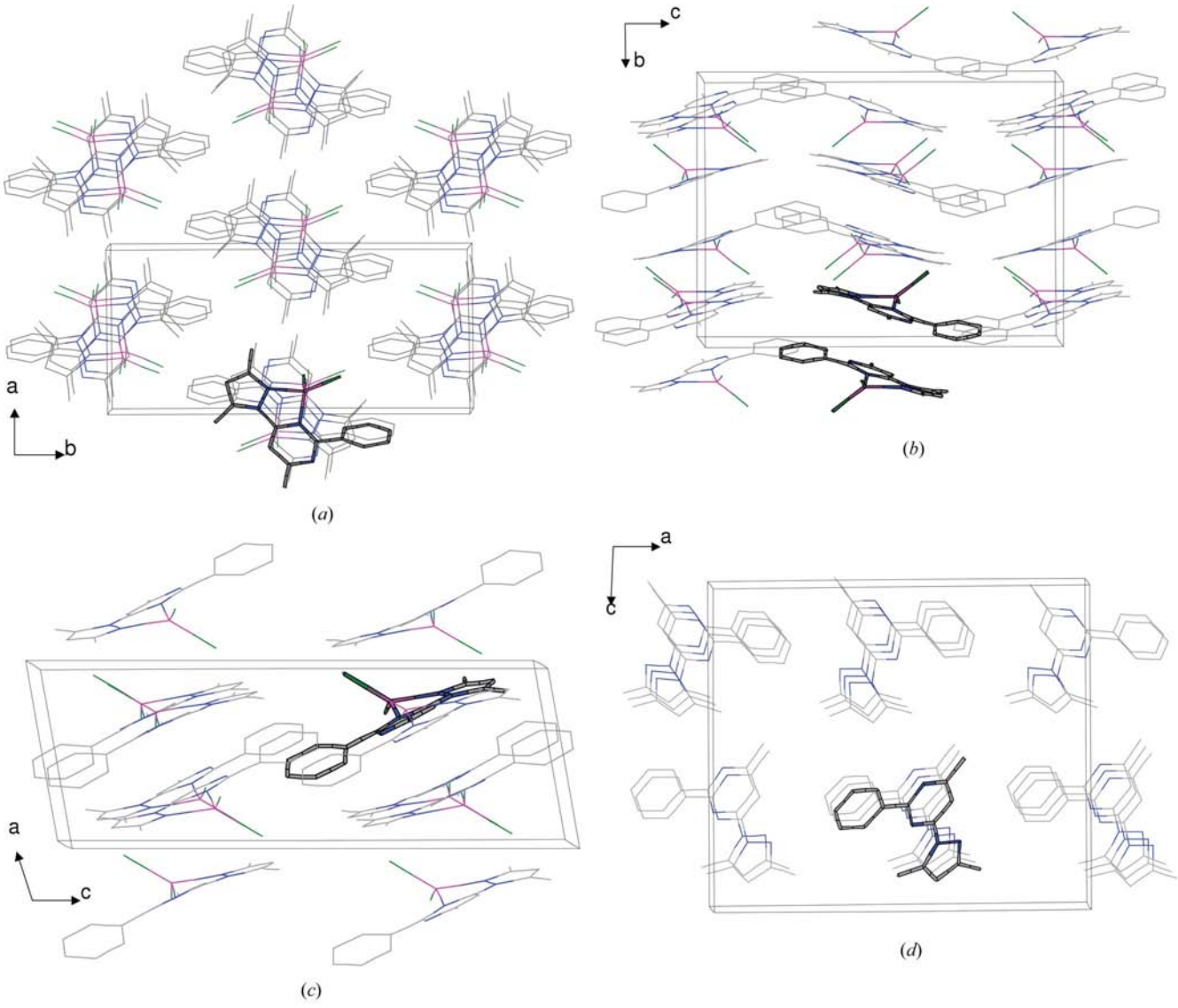

Figure 6
Crystal packings of three polymorphic modifications (*a*) (2O), (*b*) (2EG) and (*c*) (2G), and (*d*) the ligand (1).

of crystalline space. The relative efficiency of π–π stacking can therefore be estimated not by visually comparing projections of one molecule on the π-system of another (molecular overlap diagram), but by comparing the solid angles of the boundary surfaces of the molecules within π–π stacks.

In conclusion we can suppose that the possible reason for the difference in colour between the three polymorphs is the presence or absence of π–π stacking. It is interesting that when π–π interactions result in infinite stacks (2O), the density, packing coefficient and uniformity of the crystal packing notably decreases. It seems as though in this case the loss in energy of the non-directed van der Walls intermolecular interactions is compensated for by the energy of π–π stacking. To prove that it is necessary to make quantum chemical calculations together with spectroscopic measurements, which will be the subject of future investigations.

This work was financially supported by the Presidium of Russian Academy of Sciences. The authors thank Professor V. A. Blatov (Samara State University, Russia) for providing the *TOPOS* program set and Dr D.Yu. Naumov for powder diffraction measurements.

References

Bernstein, J. (1987). *Organic Solid State Chemistry*, edited by G. R. Desiraju, pp. 471–518. Amsterdam: Elsevier.
Bernstein, J. (1993). *J. Phys. D Appl. Phys.* **26**, B66–B76.
Bernstein, J., Davey, R. J. & Henck, J.-O. (1999). *Angew. Chem. Int. Ed.* **38**, 3441–3461.
Blatov, V. A (2001). *Z. Kristallogr.* **216**, 165–171.
Blatov, V. A. & Serezhkin, V. N. (2000). *Russ. J. Inorg. Chem.* **45**, Suppl. 2, S105–S222.
Blatov, V. A., Shevchenko, A. P. & Serezhkin, V. N. (2000). *J. Appl. Cryst.* **33**, 1193; http://topos.ssu.samara.ru.

Conway, J. H. & Sloane, N. J. A. (1988). *Sphere Packings, Lattices and Groups.* New York: Springer Verlag.
Druzhkov, N. O., Teplova, I. A., Glushakova, V. N., Skorodumova, N. A., Abakumov, G. A., Zhao, B., Berluche, E., Schulz, D. N., Baugh, L. S., Ballinger, C. A., Squire, K. R., Canich, J. A. M. & Bubnov, M. P. (2004). PCT Int. Appl. WO 2004007509. 22 Jan; *Chem. Abstr.* **140**, 128149 (2004).
Ejima, A., Sugimori, M. & Mitsui, I. (1996). PCT Int. Appl. WO 9610024. 4 Apr; *Chem. Abstr.* **125**, 114693 (1996).
Elguero, J., Guerrero, A., Gomez de la Torre, F., de la Hoz, A., Jalon, F. A., Manzano, B. R. & Rodriguez, A. (2001). *New J. Chem.* **25**, 1050–1060.
Escriva, E., Garcia-Lozano, J., Martinez-Lillo, J., Nunez, H., Server-Carrio, J., Soto, L., Carrasco, R. & Cano, J. (2003). *Inorg. Chem.* **42**, 8328–8336.
Fischer, R., Alig, B., Bretschneider, T., Es-Sayed, M., Erdelen, C., Loesel, P. & Reckmann, U. (2002). Ger. Offen. DE 10108480, 5 Sep; *Chem. Abstr.* **137**, 201325 (2002).
Fridman, N., Kopon, M., Sheynin, Y. & Kaftory, M. (2004). *Acta Cryst.* B**60**, 97–102.
Gavezzotti, A. & Fillippini, G. (1995). *J. Am. Chem. Soc.* **117**, 12299–12305.
Gomez de la Torre, F., de la Hoz, A., Jalon, F. A., Manzano, B. R., Rodriguez, A. M., Elguero, J. & Martinez-Ripoll, M. (2000). *Inorg. Chem.* **39**, 1152–1162.
Grote, T., Gypser, A., Rheinheimer, J., Rose, I., Schaefer, P., Schieweck, F., Sauter, H., Gewehr, M., Mueller, B., Tormo i Blasco, J., Ammermann, E., Strathmann, S., Lorenz, G. & Stierl, R. (2002). PCT Int. Appl. WO 2002074753, 26 Sep; *Chem. Abstr.* **137**, 263046 (2002).
Ikeda, M., Maruyama, K., Nobuhara, Y., Yamada, T. & Okabe, S. (1996). *Chem. Pharm. Bull.* **44**, 1700–1706.
Ikeda, M., Maruyama, K., Nobuhara, Y., Yamada, T. & Okabe, S. (1997). *Chem. Pharm. Bull.* **45**, 549–551.
Janiak, C. (2000). *J. Chem. Soc. Dalton Trans.* pp. 3885–3896.
Kitaigorodskii, A. I. (1973). *Molecular Crystals and Molecules.* New York: Academic Press.
Money, V. A., Elhaiek, J., Evans, I. R., Halcrow, M. A. & Howard, J. A. K. (2004). *Dalton Trans.* pp. 65–69.
O'Keeffe, M. (1995). *Z. Kristallogr.* **210**, 905–908.
Oshima, Y., Akimoto, T., Tsukada, W., Yamasaki, T., Yamaguchi, K. & Kojima, H. (1969). *Chem. Pharm. Bull.* **17**, 1492–1497.
Ovchinnikov, Yu. E., Potekhin, K. A., Panov, V. N. & Struchkov, Yu. T. (1995). *Dokl. Akad. Nauk*, **340**, 62–66 (In Russian).
Peresypkina, E. V. & Blatov, V. A. (1999). *Theochem.* **489**, 225–236.
Peresypkina, E. V. & Blatov, V. A. (2000*a*). *Acta Cryst.* B**56**, 501–511.
Peresypkina, E. V. & Blatov, V. A. (2000*b*). *Acta Cryst.* B**56**, 1035–1045.
Peresypkina, E. V. & Blatov, V. A. (2002). *Z. Kristallogr.* **217**, 91–102.
Sedereviciute, V., Garaliene, V., Vainilavicius, P. & Hetzheim, A. (1998). *Pharmazie*, **53**, 233–237.
Selby, T. P., Drumm, J. E., Coats, R. A., Coppo, F. T., Gee, S. K., Hay, J. V., Pasteris, R. J. & Stevenson, T. M. (2002). *Am. Chem. Soc. Symposium Series*, 800 (Synthesis and Chemistry of Agrochemicals VI), 74–84. American Chemical Society; *Chem. Abstr.* **136**, 200158 (2002).
Sheldrick, G. M. (1990). *Acta Cryst.* A**46**, 467–473.
Sheldrick, G. M. (1998). *SHELXL*97, Release 97-2. University of Göttingen, Germany.
Sneddon, S. F., Kane, J. L., Hirth, B. H., Vinick, F., Qiao, S. & Nahill, S. R. (2001). PCT Int. Appl. WO 2001087849, 22 Nov; *Chem. Abstr.* **135**, 371760 (2001).
Staveski, M. M., Sneddon, S. F., Yee, C. & Janjigian, A. (2001). PCT Int. Appl. WO 2001056974, 9 Aug; *Chem. Abstr.* **135**, 166842 (2001).
Virovets, A. V. & Podberezskaya, N. V. (1992). *Kristallografiya*, **37**, 1017–1019 (in Russian).
Wells, A. F. (1986). *Structural Inorganic Chemistry*, 5th Ed., p. 8. Oxford: Clarendon Press.
Yoshino, M., Takahashi, K., Okuda, Y., Yoshizawa, T., Fukushima, N. & Naoki, M. (1999). *J. Phys. Chem. A*, **103**, 2775–2783.
Yu, L., Stephenson, G. A., Mitchell, C. A., Bunnell, C. A., Snorek, S. V., Bowyer, J. J., Borchardt, T. B., Stowell, J. G. & Byrn, S. R. (2000). *J. Am. Chem. Soc.* **122**, 585–591.
Yu, L. (2002). *J. Phys. Chem. A*, **106**, 544–550.
Yu, L., Reutzel-Edens, S. M. & Mitchell, C. A. (2000). *Org. Prcoess Res. Dev.* **4**, 396–402.
Zefirov, Yu. V. (1997). *Crystallogr. Rep.* **42**, 111–116.